Optimized Processing Of Quantitative Susceptibility Mapping-Based Gadolinium Perfusion MRI: Correction Of Bulk Susceptibility Effects And Comparison of Arterial Input Function Selection From ΔR_2^* and QSM Data

David Bonekamp[1], Xu Li[1,2], Richard Leigh[3], Peter C. van Zijl[1,2], and Peter B. Barker[1,2]

[1]The Russell H. Morgan Department of Radiology and Radiological Science, Johns Hopkins University, Baltimore, Maryland, United States, [2]FM Kirby Research Center for Functional Brain Imaging, Kennedy Krieger Institute, Baltimore, Maryland, United States, [3]Neurology, Johns Hopkins University, Baltimore, Maryland, United States

Target Audience. Researchers and clinicians working with MR perfusion imaging. **Purpose.** Analysis of dynamic MRI during bolus injection of Gd contrast agent is traditionally performed by repeated measurement of brain signal relaxation times (usually T_2*) to estimate Gd concentration, however a nonlinear relationship between ΔR_2* and Gd tissue concentration has been reported[1,2]. Quantitative Susceptibility Mapping (QSM) estimates the tissue susceptibility distribution $\Delta\chi(\mathbf{r})$ from the MR phase data[3,4]. $\Delta\chi$ is expected to represent a different contrast mechanism and to be less affected by nonlinearities in the estimation of the Gd concentration (molar susceptibility χ_m). In our previous work[5], we have demonstrated the feasibility of dynamic QSM data $\Delta\chi(\mathbf{r},t)$ reconstruction for the measurement of cerebral blood flow (CBF). This abstract presents a refined QSM-based analysis scheme which addresses bulk Gd effects, and compares QSM and ΔR_2*-based analyses. The influence of arterial input function (AIF) selection from both the QSM data and the ΔR_2* data is also investigated. **Methods.** *Experiment.* A 68 year-old male patient without perfusion deficit was scanned at 3.0T (Philips Healthcare) as part of his stroke workup for symptoms of blurred vision. Informed consent and IRB approval were obtained; *Scan parameters.* 20 slices, 80 dynamics, multi-slice 2D gradient echo EPI, FOV=240x240 mm^2, 256x256 matrix, 5mm slice thickness, TR/TE 1500/40 msec, 0.2 mmol/kg Gd bolus. *Analysis.* Perfusion analysis utilized the magnitude data to determine ΔR_2*(t)[6]. QSM processing included Laplacian phase unwrapping[7,8], frequency map calculation f(t), background field removal (dipole fitting) and susceptibility calculation (LSQR method)[3,7]. Compared to the previously presented[5] data (to effectively avoid artificial susceptibility decrease in brain voxels during bolus passage), the $\Delta\chi$(t) maps were corrected by adding the average background susceptibility change estimated from the dipole fitting analysis before perfusion processing. This step is necessary to account for bulk Gd effects which would otherwise be removed with the background. Perfusion parameters (CBF, CBV and MTT) were calculated using standard perfusion processing[6] with Tikhonov regularization[9], using both ΔR_2*(t) and $\Delta\chi$(t) maps. Two semi-automatically detected arterial input functions (AIF)[10] were determined: a QSM-derived AIF used for QSM processing only, and a DSC-derived AIF applied to both analyses. Due to dynamic range and aliasing, the QSM-derived AIF shape was determined from voxels adjacent to the MCA and scaled to the expected peak concentration by the use of a scaling factor determined from the equilibrium concentration. Quantitative analysis used a transverse relaxivity of Gd r_2=5.2 L•mmol^{-1}•sec^{-1} and molar susceptibility χ_m=0.3209•10^{-3} L•mol^{-1} for quantitative conversion[2,11]. **Results.** Fig. 1 depicts the perfusion parameter maps for CBF, CBV and MTT determined with ΔR_2* and QSM (for both AIF choices). QSM-derived perfusion shows comparable data quality and demonstrates good general qualitative and quantitative agreement to DSC data. While CBF results are most similar, both CBV and MTT show decreased values in WM for QSM-derived maps. Fig.2 depicts the DSC-derived AIF (Fig.2a) and the QSM-derived AIF (Fig.2b). Both were converted into units of mM of Gd. QSM and ΔR_2*-derived AIF are of comparable quality and show good quantitative agreement. **Discussion.** An improved processing scheme of QSM perfusion data achieves comparable data quality to DSC. QSM may have decreased sensitivity to slowly perfused WM due to SNR limitations (currently, respiratory and extracranial Gd related phase changes cannot be fully eliminated). Local differences in the observed WM and GM perfusion may reflect different microvascular sensitivities of both methods, as the underlying contrast mechanism of ΔR_2* exploits the dephasing related signal amplitude loss, while QSM is based on the average detected local resonance frequency. Thus, QSM may add complementary information to MR perfusion data, while both ΔR_2* and QSM perfusion are characterized by a sensitivity dominated by large vessels. Despite SNR limitations, the QSM-derived AIF shape and peak is very similar to the ΔR_2*-derived AIF. QSM-AIF calculation currently requires a scaling factor estimated from the steady state susceptibility change. **Conclusion.** A refined processing scheme for QSM perfusion analysis identifies and addresses bulk Gd susceptibility changes and leads to good agreement to DSC perfusion parameters. Separation of background from contrast-induced phase changes remains a challenge. Some of the QSM perfusion information may be complementary to ΔR_2*. Accurate AIF curves can be determined from the QSM data, and QSM- and ΔR_2*-derived AIF yield comparable perfusion results.

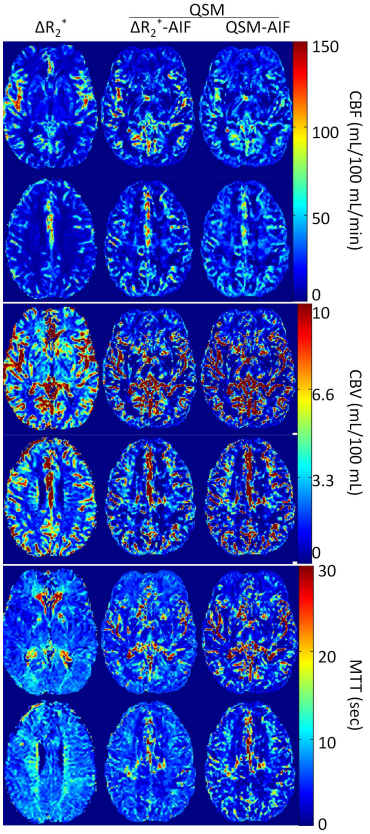

Figure 1

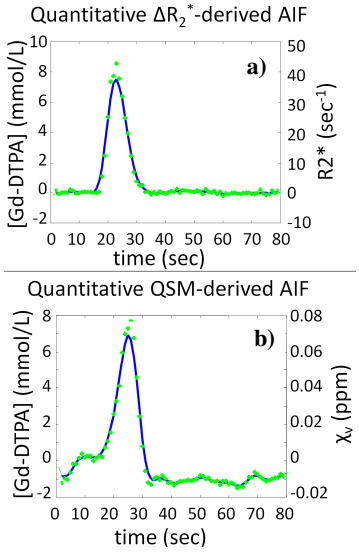

Figure 2

References. *1.* F Calamante, et al. Magn Reson Med. 58:544-53, 2007. *2.* MJ van Osch, et al. Magn Reson Med. 49:1067-76, 2003. *3.* W Li, et al. Neuroimage. 55:1645-56, 2011. *4.* F Schweser, et al. Neuroimage. 54:2789-807, 2011. *5.* D Bonekamp, et al. Proc Int Soc Magn Reson Med, pg. 1937, 2011. *6.* L Ostergaard, et al. Magn Reson Med. 36:715-25, 1996. *7.* L de Rochefort, et al. Magn Reson Med. 63:194-206, 2010. *8.* S Wharton, et al. Magn Reson Med. 63:1292-304, 2010. *9.* S Sourbron, et al. Phys Med Biol. 49:3307-24, 2004. *10.* L Knutsson, et al. Magn Reson Imaging. 28:1-7, 2010. *11.* J Pintaske, et al. Invest Radiol. 41:213-21, 2006.

Funding. NIH P41 EB015909.